

NASA Technical Memorandum 102481

# A Fiber Optic Sensor for Noncontact Measurement of Shaft Speed, Torque and Power

George C. Madzsar  
*Lewis Research Center*  
*Cleveland, Ohio*

Prepared for the  
36th International Instrumentation Symposium  
sponsored by the Instrument Society of America  
Denver, Colorado, May 6-10, 1990

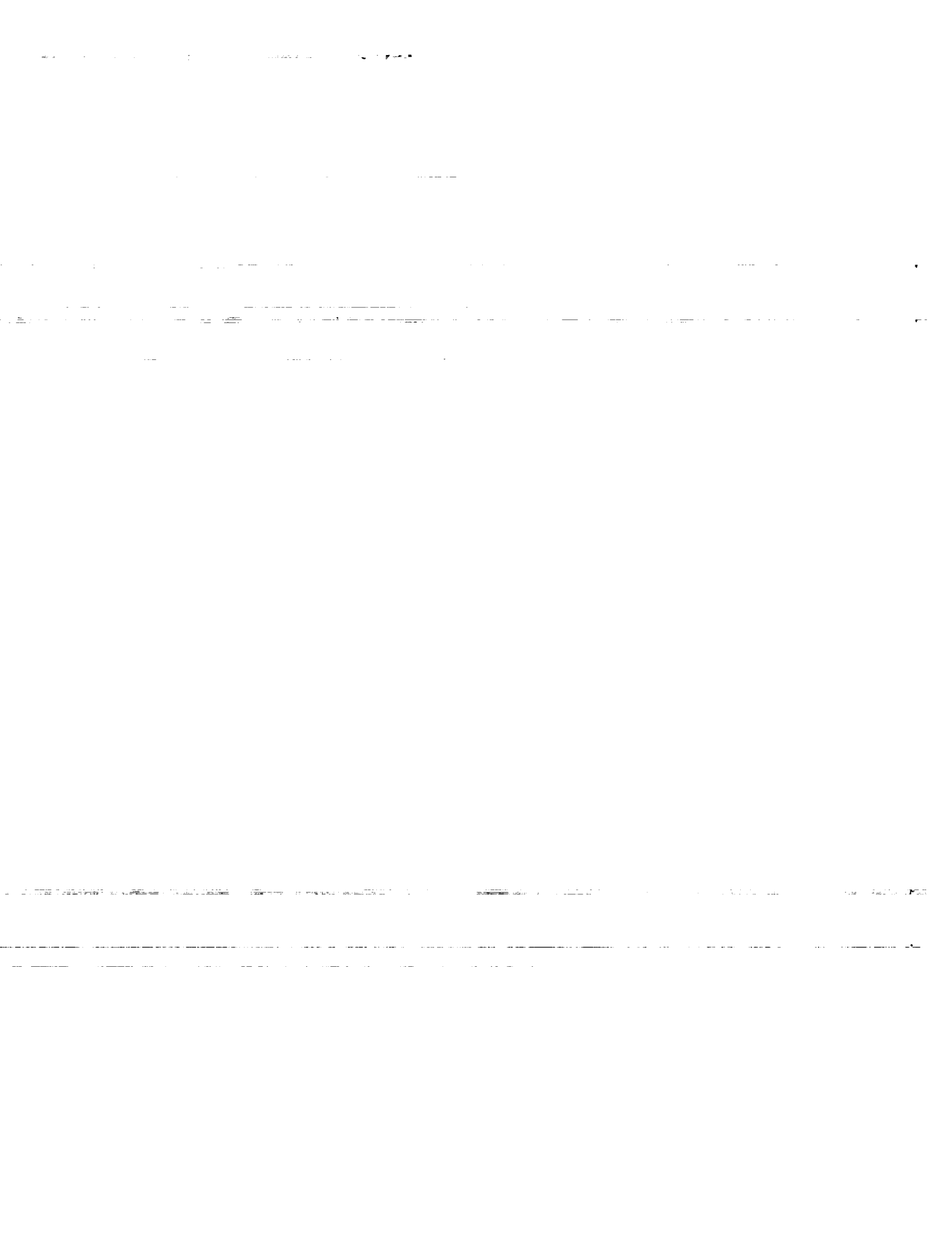


(NASA-TM-102481) A FIBER OPTIC SENSOR FOR  
NONCONTACT MEASUREMENT OF SHAFT SPEED,  
TORQUE, AND POWER (NASA) 11 p CSCL 14B

N90-21360

Unclass

G3/35 0277365



A FIBER OPTIC SENSOR FOR NONCONTACT MEASUREMENT OF SHAFT SPEED,  
TORQUE AND POWER

George C. Madzsar  
National Aeronautics and Space Administration  
Lewis Research Center  
21000 Brookpark Road  
Cleveland, Ohio 44135

ABSTRACT

E-5271  
A fiber optic sensor which enables noncontact measurement of the speed, torque and power of a rotating shaft has been fabricated and tested. The sensor provides a direct measurement of shaft rotational speed and shaft angular twist, from which torque and power can be determined. Angles of twist between 0.005 and 10° have been measured. Sensor resolution is limited by the sampling rate of the analog to digital converter, while accuracy is dependent on the spot size of the focused beam on the shaft. Increasing the sampling rate improves measurement resolution, and decreasing the focused spot size increases accuracy. Digital processing allows for enhancement of an electronically or optically degraded signal.

INTRODUCTION

In order to determine the health and control the performance of rotating machinery, knowledge of its speed, torque and power are required. For high-performance turbopumps such as those used on pump fed liquid propellant rocket engines, rotational speed could be the controlling parameter for turbopump operation, since speed control provides a means for controlling pump volumetric flow. Torque measurements provide information regarding bearing and seal condition. A change in torque without a corresponding change in speed indicates changes in the condition of these components. Measurement of turbopump power provide information regarding its efficiency, which is related to the condition of the rotors and stators.

Rotational speed can be measured by many methods. Common methods include sensors based on magnetic, inductive, capacitive, or optical principles. These techniques, excluding the optical, exhibit nonlinear behavior at the cryogenic temperatures which are typical of a rocket engine environment. Torque is typically determined using a strain gauge which is bonded to the shaft, and relating the measured strain to the applied torsional load. The drawback to this type of sensor is that slip rings or telemetry techniques are required to transfer the strain signal from the spinning shaft. At high rotational speeds and at cryogenic temperatures, these signal transfer

techniques can be difficult to incorporate. Shaft power is not measured directly, rather it is calculated as the product of angular velocity and torque.

Currently on the space shuttle main engines (SSME) speed is measured on the low pressure fuel turbopump, the low pressure oxidizer turbopump, and the high pressure fuel turbopump (HPFTP) during engine operation. Speed is not measured on the high pressure oxidizer turbopump (HPOTP). Torque and power are not measured during SSME operation. Figure 1 displays the SSME HPOTP.

This paper documents the development of a prototype noncontact speed, torque and power sensor for turbopump applications. The sensor could be located between the individual turbopump rotors to measure torque and power of each stage, or across the entire shaft, measuring overall turbopump performance. Table I displays the key performance parameters of a Phase II HPOTP. With this sensor, some of these parameters could be monitored or derived during engine operation.

This sensor is different from previous fiber optic speed, torque and power sensors (1,2) in that raw data from which the various parameters are calculated is analyzed as a group of data points rather than as a stream of individual data points. Data analysis in this fashion allows for computer enhancement of a signal that may have been corrupted by either nontransparent impurities in the optical path, beam unfocus caused by shaft orbit, or view of the shaft through multiple phase fluids. The disadvantage of this analysis technique is that speed, torque and power cannot be determined in real time. The appropriate number of data samples must be collected and transferred to the computer prior to digital signal enhancement and parameter calculation. This requirement, along with the fact that digital manipulations require a finite amount of computer time, limit the sensor to non-real time applications.

SENSOR DESCRIPTION

A schematic drawing of the sensor is shown in figure 2. A beam from a helium neon laser is coupled into a single strand, multimode optical

fiber. A fiber optic bidirectional coupler splits the beam into two paths. At the ends of the fibers are 0.29 pitch gradient index (GRIN) lenses, which focus the light onto the shaft. The GRIN lenses are placed at the proper distance from the shaft so that the focal point of the beam is at the surface of the shaft (fig. 3). The use of monochromatic light assures a small spot size by minimizing chromatic aberration. A single light source is used since it minimizes the number of components, and cancels the effects of intensity fluctuations in the source.

A pair of reflective elements are mounted to the shaft as shown in figures 2 and 3. As the shaft rotates, these sections pass in front of the focused beam, and reflect the incident light. The reflected light is focused by the same GRIN lens back into the fiber. Through bidirectional couplers, the reflected light is transmitted to a pair of photodiodes. The signals which are monitored by the photodiodes are digitized by an analog to digital converter (ADC), and transferred to a microprocessor for analysis.

The test rig utilized in these experiments consisted of a 0.25 hp motor spinning a 0.5 in. diameter, 48 in. long Bakelite shaft at 1180 rpm. The shaft was supported by three pillow block bearings. Shiny metallic fittings fabricated from stainless steel covering 0.125 in. of the shaft circumference were clamped to the shaft 40 in. apart. Intensity of the reflected light was monitored with a pair of high speed photodiodes. The photodiodes were electrically connected to a digital storage oscilloscope, which digitized the signals. To assure a common time base for the measurements, both channels of the oscilloscope were triggered simultaneously by the rising leading edge of the reflection signal from the reflective section closest to the motor. When the oscilloscope was triggered, 8192 voltage measurements corresponding to optical intensity as a function of time were recorded from each photodiode. The memory depth of the oscilloscope was 8192 readings per channel. The time increment between intensity measurements was determined by the digitization rate of the ADC in the oscilloscope, which was variable up to the maximum rate of  $1 \times 10^9$  samples per second.

It should be noted that SSME turbopump shafts are polished and naturally reflect light. A highly reflective shaft surface could be accommodated by this sensor by darkening sections of it, and determining the time delays from the passage of the reflective and nonreflective sections. The sensor requires that a distinct interface exists between reflective and nonreflective sections on the circumference of the shaft.

#### EXPERIMENTAL PROCEDURE

The sensor signals were analyzed and the appropriate calculations performed with a microcomputer. A torsional load was applied to the free end of shaft with friction.

The recorded signals from the sensor were enhanced using digital signal processing techniques. As a minimum, a low pass filter was applied to the raw data in order to smooth the waveforms, thereby enabling a more accurate determination of when in time the edge of the reflective elements passed in front of the lens. If the reflection signals are corrupted by influences such as nontransparent impurities in the optic path, beam unfocus caused by orbital movements of the shaft, or view of the shaft through multiple phase fluids, manipulation routines such as curve fitting or point extrapolation could be incorporated to minimize errors.

A scheme that can be used to determine the time at which the reflective element passed under the sensor optics consists of point extrapolation based on the slope of the rising edge of the reflected light pulse. Digitized data points corresponding to intensity of the reflected light are stored as an array in the computer memory. An algorithm, implemented in software, searches the array for the rising edge of the reflected light pulse. Upon finding the edge, its slope is determined, and from the slope, the point in time at which the rise began is extrapolated. This technique maintains sensor accuracy during optical degradation(s) that cause nonconstant rise times and/or variations in the peak amplitude of the reflected light. These degradations include beam focus changes, or partial blockage of the optic path.

Shaft rotational speed is determined from the time delay between consecutive pulses of reflected light from a reflective element. Torque is determined from the angular twist of the shaft. Twist is calculated as the product of speed and the time delay between reflected light pulses from the two reflective elements. Power is determined as the product of angular velocity and torque.

The theoretical resolution of the speed and twist measurement is a function of the rate at which the intensity of the reflected light is sampled. Resolution of the speed is determined in the following manner: Figure 4 displays discrete measurements of the reflected light intensity as a function of time from one of the reflective sections as the shaft rotates. Since there is one reflection per revolution, the time per revolution is the time between the two pulses in the figure. The digitized intensity measurements are analyzed by a computer, which "observes" the passage of the reflective element at time  $t_1$ . In actuality, the edge of the reflective element passed under the lens at a time between  $t_1$  and  $(t_1 - dt_1)$ , where  $dt_1$  is the time between samples. After completing one revolution, the reflective element again passes under the lens at a time between  $t_1'$  and  $(t_1' - dt_1)$ . With respect to figure 4, the minimum possible time for one revolution can be expressed as  $(t_1' - dt_1) - t_1$ , which can be rewritten as  $(t_1' - t_1) - dt_1$ . The maximum possible time for one revolution is  $t_1' - (t_1 - dt_1)$ , or  $(t_1' - t_1) + dt_1$ . Therefore, the speed measurement can be expressed as:

$$w = \frac{1}{(t_1' - t_1) \pm dt_1} \quad (1)$$

where

w = rotational speed (revolutions/second)  
t<sub>1</sub> = time of initial reflective element passage (seconds)  
t<sub>1</sub>' = time of next reflective element passage (seconds)  
dt<sub>1</sub> = time between samples during speed measurement (1/sampling rate)

From the difference between the minimum and maximum possible speed values calculated using equation 1, the following equation for measurement uncertainty can be derived:

$$dw = \frac{dt_1}{(t_1' - t_1)^2 - dt_1^2} \quad (2)$$

where

dw = rotational speed uncertainty (revolutions/second)  
t<sub>1</sub> = time of initial reflective element passage (seconds)  
t<sub>1</sub>' = time of next reflective element passage (seconds)  
dt<sub>1</sub> = time between samples during speed measurement (1/sampling rate)

From equations 1 and 2, the following expression for the speed measurement can be derived:

$$w \pm dw = \frac{1}{(t_1' - t_1) \pm dt_1} = \frac{dt_1}{(t_1' - t_1)^2 - dt_1^2} \quad (3)$$

Shaft twist, caused by torsional load, is the product of the speed and the time delay between pulses of reflected light from the two reflective elements on the shaft. This can be calculated using the following equation:

$$\phi \pm d\phi = (w \pm dw)[(t_2 - t_1) \pm dt_2] \quad (4)$$

where

φ = angle of shaft twist (radians)  
w = rotational speed (revolutions/second)  
dw = speed uncertainty (revolutions/second)  
t<sub>1</sub> = time of passage of one reflective section (seconds)  
t<sub>2</sub> = time of passage of other reflective section (seconds)  
dt<sub>2</sub> = time between samples during twist measurement (1/sampling rate)

Using logic similar to that in the development of the speed uncertainty, it can be shown that the theoretical resolvable angular twist of the shaft may be calculated from the following equation

$$\phi \pm d\phi = \frac{(t_2 - t_1)}{(t_1' - t_1)} \pm \frac{(t_1' - t_1)dt_2 + (t_2 - t_1)dt_1}{(t_1' - t_1)^2 - dt_1^2} \quad (5)$$

where

dφ = angular uncertainty (radians)

From the solution to equation 3, speed can be expressed as  $w \pm dw$  revolutions per second. From the solution to equation 5, twist can be expressed as  $\phi \pm d\phi$ . It can be seen from equation 3 that the theoretical resolution of the speed measurement is a function of the sampling rate only, as expected. The resolution of the twist measurement in equation 4 is a function of the speed measurement resolution and the sampling rate used during twist measurement. Increasing the sampling rate allows for measurement of greater speeds and/or less twist without a degradation in resolution. Note that dt<sub>1</sub> is the inverse of the sampling rate used for the speed measurement, and dt<sub>2</sub> is the inverse of the sampling rate used for the twist measurement. If the same sampling rate is used for both measurements, dt<sub>1</sub> = dt<sub>2</sub>.

For these experiments, a rate of 50 000 samples per second was used for the speed measurements. With respect to the rotational speed of 1180 rpm and equation 3, the theoretical resolution is 1180±0.464 rpm. The sampling rate for measurement of the shaft twist was 2,500,000 samples per second. With respect to equation 5, the minimum twist that can be measured is 0.00045°, with an uncertainty of ±4.51×10<sup>-4</sup>°.

To relate the calculated theoretical resolution of this sensor to a more realistic turbopump configuration, consider the following example: A turbopump with the power equal to 30 000 hp spins at 30 000 rpm, consists of one turbine and one pump rotor separated by 6 in. The rotors are mounted on a hollow shaft with a 1.00 in. outer radius and 0.50 in. inner radius. The shaft is fabricated from a high strength steel alloy that has a modulus of rigidity equal to 11.5×10<sup>6</sup> psi. From the speed and power values, the torque is calculated to be 6.303×10<sup>4</sup> in. - lbs. Based on the shaft physical dimensions, modulus of rigidity, and the calculate torque, the maximum shaft twist is calculated to be 3.72×10<sup>-2</sup> rad, or 2.13°. Using a sampling rate of 1×10<sup>6</sup> samples per second for both the speed and twist measurements, speed is calculated to be 30 000±0.250 rpm, and twist equal to 2.1486±0.0297°.

## RESULTS

Initial tests were performed to determine resolution, sensitivity and accuracy of the optical hardware and analysis software. During testing, angles of shaft twist between 0.005 and 10° were measured.

The time resolution of when the reflective surface passes in front of the beam is related to the sampling rate of the analog to digital converter. Increasing the sampling rate allows for greater resolution due to increased frequency response. The ideal sampling rate is dependent on the speed of shaft rotation, the desired resolution, and the memory depth of the digital storage device.

The recorded waveforms required low pass filtering to smooth out the signal. The intensity of the

reflected light was extremely irregular due to imperfections on the surface finish of the reflective elements, eccentricity of the shaft, and shaft orbit during rotation. Figures 5 and 6 display unfiltered and filtered reflection signals, respectively. As can be seen, low pass filtering removes the high frequency fluctuations. Even with filtering, the signal is not the symmetric square wave shape that is expected from the reflective element. Pulse symmetry is not critical for the determination of when in time the reflective elements pass in front of the optics and reflect light. Also, imperfect surface conditions do not present a problem since the signals derived from these surfaces are consistent regardless of rotational speed. For these experiments, the reflective elements were considered fully under the lens when the reflected intensity was 40 percent of the maximum measured reflected intensity.

Accuracy of the sensor is maximized when the spot size on the reflective sections of the shaft is minimized. This can be seen from figures 7 and 8. Figure 7 displays the amplitude of the reflected light versus time with the focal point of the beam approximately 2 mm above the surface of the reflective element. Figure 8 displays the signal with the beam focused onto the reflective element. Differences in the rise time and signal amplitude can readily be seen. Minimizing the spot size causes light that is reflected to emanate from an extremely small spot, resulting in a sharper rise in reflected light intensity as the edge passes through the focal point of the beam. This enables greater accuracy in determining the time when an edge passes beneath the lens.

Figure 9 displays the intensity of the reflected light versus time for one of the reflective sections. The two peaks in the figure correspond to the reflective elements passing in front of the optics and reflecting light during shaft rotation. Shaft speed is calculated as  $1/(t1' - t1)$ , where  $t1$  and  $t1'$  are the times when the reflective element passes in front of the optics.

Figure 10 displays the intensity of the reflected light versus time from the two reflective sections as a torsional load is applied to the spinning shaft. The two waveforms correspond to the passage of the two reflective elements. The time delay between the signals is caused by shaft angular twist. The amount of twist is calculated using equation 2. Torque is proportional to twist.

## FUTURE EFFORTS

Future efforts in the development of this sensor include calibration against a standard torque meter with a known load. Following that, work will be performed to determine the effects of optical interference such as nontransparent impurities in the optic path, and viewing the shaft through multiple phase fluids. Work will also be performed to determine the effects of shaft orbital travel, which results in an unfocused beam. The digital enhancement algorithms will be tested and evaluated to determine the extent of optical interference can be tolerated before the uncertainty of the speed, torque and power measurements become excessive.

## CONCLUSION

A fiber optic sensor to measure shaft rotational speed, torque and power was fabricated. Testing indicated that measurement resolution improves with increasing sampling rate of the analog to digital converter. The maximum speed, and the torque induced shaft twist that can be measured is also limited by the sampling rate. Accuracy of the sensor is greatest when the spot size of the focused beam on the shaft is minimized. Digital filtering is required to smooth out the pulse shape prior to parameter calculations. Digital enhancement algorithms can be used to correct for optical interference.

## REFERENCES

1. Rudd, R.E.; Kline, B.R.; Hoff, F.G.; and Spillman, W.B.: Fiber Optic Torquemeter Design and Development. International Instrumentation Symposium, 34th, Proceedings, Instrument Society of America, Research Triangle Park, NC, 1988, pp.199-204.
2. Lesco, D.J.; Buchele, D.R.; and Oberle, L.G.: A Digital Optical Torquemeter for High Rotational Speed Applications. NASA TM-82914, 1982.

**TABLE 1. Phase II High Pressure Oxidizer Turbopump Key Performance Parameters**

	100%		109%	
	MAIN	BOOST	MAIN	BOOST
Pump Inlet Flowrate (lb/sec)	1072.1	109.1	1162.5	125.8
Pump Inlet Pressure (Psia)	379.9	3992.2	392.3	4428.7
Pump Disch Pressure (Psia)	4118.4	7210.9	4578.2	7935.9
Pump Efficiency	.686	.808	.681	.805
Turbine Flowrate (Lb/sec)	58.8		65.49	
Turbine Inlet Pressure (Psia)	5020.0		5631.6	
Turbine Inlet Temp (R)	1522.5		1625.4	
Turbine Pressure Ratio	1.513		1.547	
Turbine Efficiency	.759		.769	
Turbine Speed (RPM)	27,263		29,194	
Turbine Horsepower	23,068		28,229	

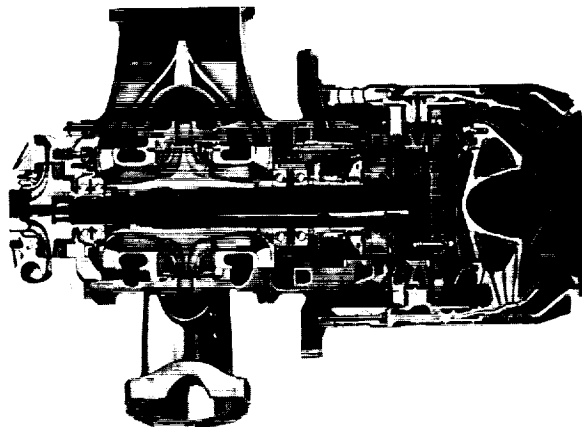


**Figure 1. High Pressure Oxidizer Turbopump of the Space Shuttle Main Engine.**

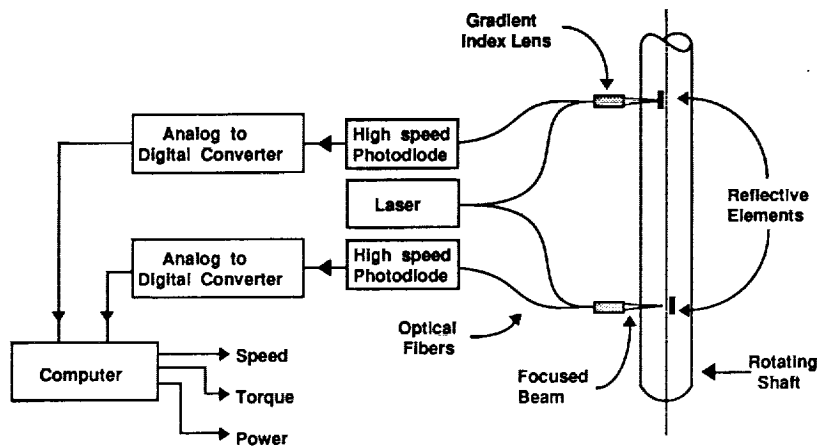


Figure 2. Schematic diagram of sensor. Misalignment of reflective sections on shaft caused by and proportional to torque induced elastic deformation.

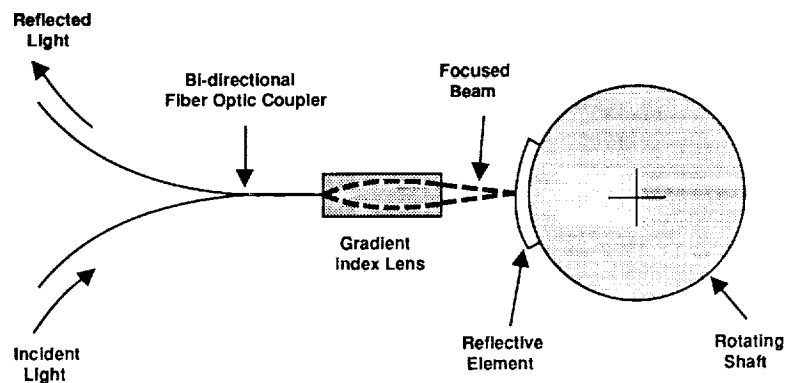


Figure 3. Gradient index lens focus the fiber transmitted light onto the shaft, and coupling the reflected light back into optical fiber.

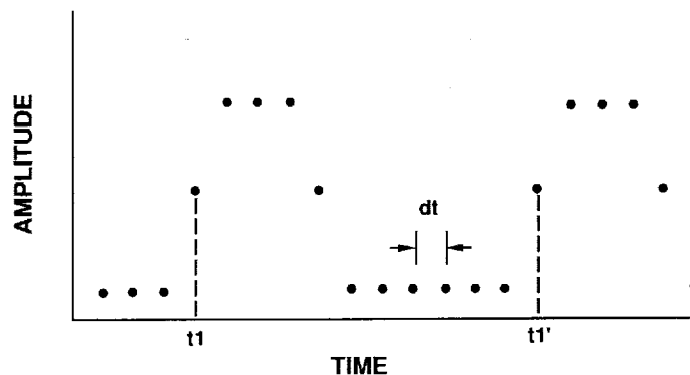
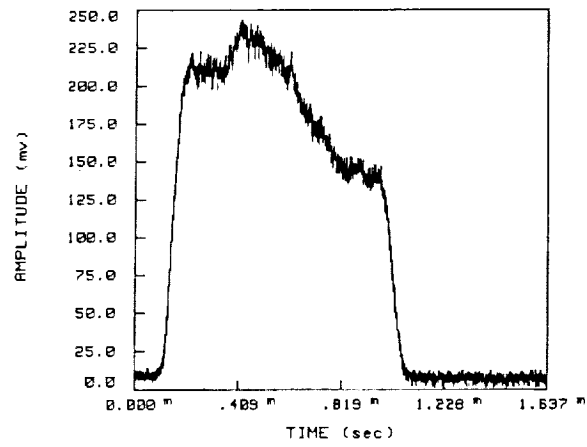
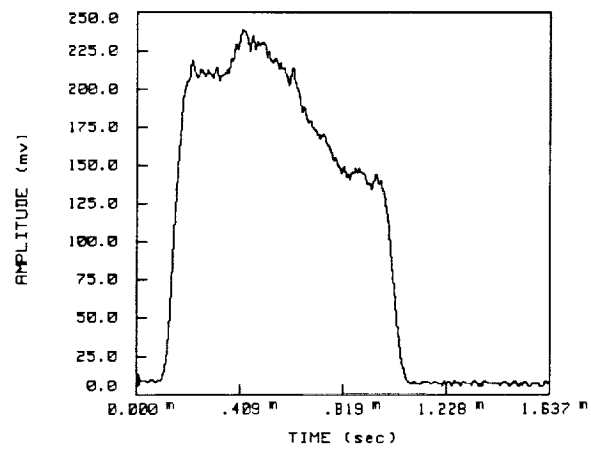


Figure 4. Discrete intensity measurements of reflected light as a function of time from one of the reflective elements. The computer "sees" the intensity increases at times  $t_1$  and  $t_1'$ . The actual increase indicated at  $t_1$  occurred between  $(t_1 - dt)$  and  $t_1$ .





**Figure 5. Intensity of reflected light as a function of time without low pass filtering**



**Figure 6. Intensity of reflected light as a function of time with low pass filtering**

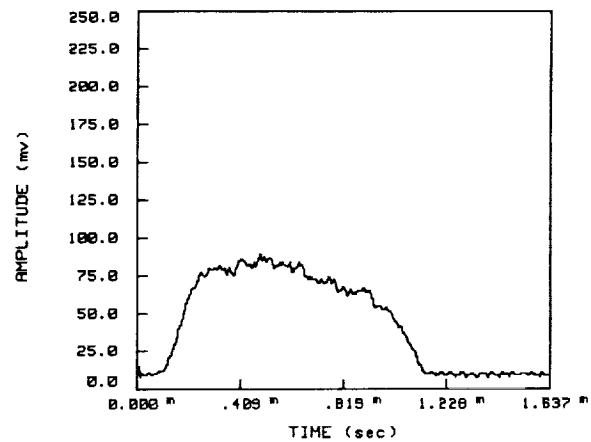


**Figure 7. Intensity of reflected light as a function of time with the beam focused above the surface of the shaft.**

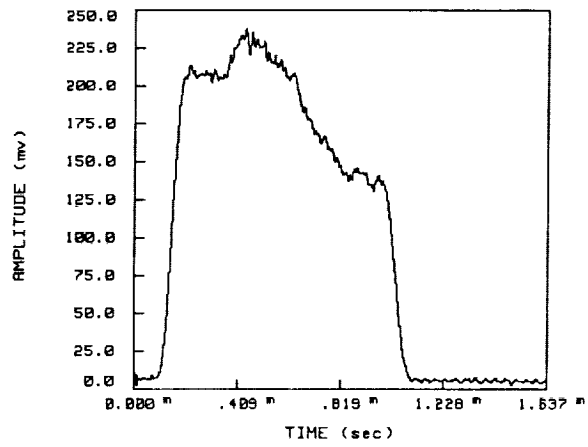


Figure 8. Intensity of reflected light as a function of time with the beam focused on the surface of the shaft.

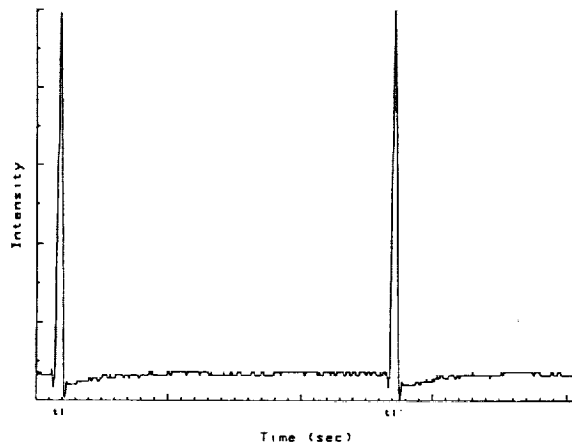


Figure 9. Intensity of reflected light as a function of time from one of the reflective sections. Shaft speed is determined from  $1/(t1' - t1)$ .

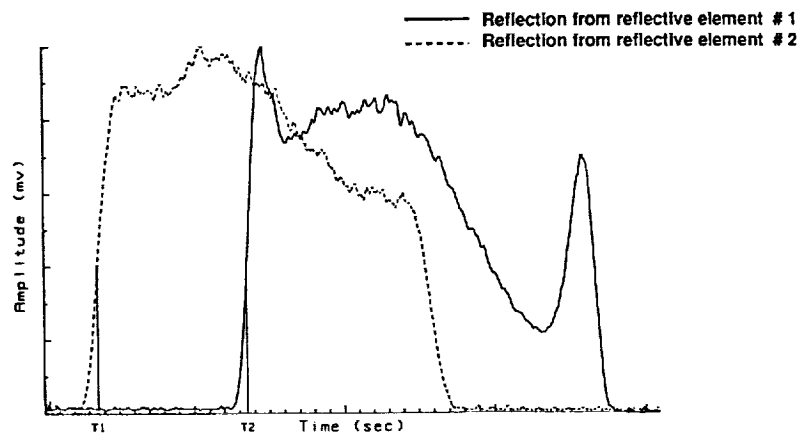


Figure 10. Time displacement of reflected light pulses is a measure of torque induced shaft twist.

$$\begin{aligned}\text{Twist} &\propto (\text{Speed})(T_2 - T_1) \\ \text{Torque} &\propto \text{Twist} \\ \text{Power} &\propto (\text{Torque})(\text{Speed})\end{aligned}$$

1. Report No. NASA TM-102481		2. Government Accession No.		3. Recipient's Catalog No.	
4. Title and Subtitle A Fiber Optic Sensor for Noncontact Measurement of Shaft Speed, Torque and Power				5. Report Date	
				6. Performing Organization Code	
7. Author(s) George C. Madzsar				8. Performing Organization Report No. E-5271	
				10. Work Unit No. 590-21-41	
9. Performing Organization Name and Address National Aeronautics and Space Administration Lewis Research Center Cleveland, Ohio 44135-3191				11. Contract or Grant No.	
				13. Type of Report and Period Covered Technical Memorandum	
12. Sponsoring Agency Name and Address National Aeronautics and Space Administration Washington, D.C. 20546-0001				14. Sponsoring Agency Code	
15. Supplementary Notes Prepared for the 36th International Instrumentation Symposium sponsored by the Instrument Society of America, Denver, Colorado, May 6-10, 1990.					
16. Abstract  A fiber optic sensor which enables noncontact measurement of the speed, torque and power of a rotating shaft has been fabricated and tested. The sensor provides a direct measurement of shaft rotational speed and shaft angular twist, from which torque and power can be determined. Angles of twist between 0.005 and 10° have been measured. Sensor resolution is limited by the sampling rate of the analog to digital converter, while accuracy is dependent on the spot size of the focused beam on the shaft. Increasing the sampling rate improves measurement resolution, and decreasing the focused spot size increases accuracy. Digital processing allows for enhancement of an electronically or optically degraded signal.					
17. Key Words (Suggested by Author(s)) Speed measurement; Torque measurement; Power measurement; Fiber optic; Sensors; Measurement				18. Distribution Statement Unclassified - Unlimited Subject Category 35	
19. Security Classif. (of this report) Unclassified		20. Security Classif. (of this page) Unclassified		21. No. of pages 10	
				22. Price* A02	